ANZIAM J. (First published online 2024), page 1 of 10*
doi:10.1017/S1446181124000166
*Provisional—final page numbers to be inserted when paper edition is published

FURTHER ACCURACY VERIFICATION OF A 2D ADAPTIVE MESH REFINEMENT METHOD USING STEADY FLOW PAST A SQUARE CYLINDER

R. LAL[1] and Z. LI[2]

(Received 27 November, 2023; accepted 7 June, 2024)

Abstract

The study applies a two-dimensional adaptive mesh refinement (AMR) method to estimate the coordinates of the locations of the centre of vortices in steady, incompressible flow around a square cylinder placed within a channel. The AMR method is robust and low cost, and can be applied to any incompressible fluid flow. The considered channel has a blockage ratio of 1/8. The AMR is tested on eight cases, considering flows with different Reynolds numbers ($5 \leq Re \leq 50$), and the estimated coordinates of the location of the centres of vortices are reported. For all test cases, the initial coarse meshes are refined four times, and the results are in good agreement with the literature where a very fine mesh was used. Furthermore, this study shows that the AMR method can capture the location of the centre of vortices within the fourth refined cells, and further confirms an improvement in the estimation with more refinements.

2020 *Mathematics subject classification*: primary 65N50; secondary 35Q30, 68U20.

Keywords and phrases: two-dimensional flow over square cylinder, adaptive mesh refinement, centre of vortices.

1. Introduction

In the domain of computational fluid dynamics (CFD), the pursuit of simulating complex fluid flows with high accuracy and efficiency has been a driving force behind technological advancements in various industries, from aerospace and automotive engineering to environmental science and biomedical research. However, fine discrete

[1]School of Mathematical and Computing Sciences, Fiji National University, Lautoka, Fiji;
e-mail: rajnesh.lal@fnu.ac.fj
[2]School of Computing and Mathematics, Charles Sturt University, Thurgoona, NSW 2640, Australia;
e-mail: jali@csu.edu.au

computational meshes are often used to develop accurate numerical solutions for CFD problems using high-performance computing. Accurate numerical solutions usually require higher-order discretization schemes for complex partial differential equations, which are prone to produce oscillations [10].

An important technique that has revolutionized the capabilities of complex CFD simulations, to improve the efficiency of flow solvers and the accuracy of numerical solutions, is adaptive mesh refinement (AMR). AMR is a computational approach that enables users to optimize their simulations by dynamically adjusting the resolution of the computational mesh in response to evolving flow features and phenomena, and reducing the computational cost [15].

Early studies in the field of adaptive mesh refinement for CFD problems can be traced to the 1980s and 1990s, including the works of Berger and Oliger [4], Bell et al. [2], Friedel et al. [9], and Berger and Leveque [3]. The development of AMR has continued to evolve with advancements in numerical methods, computer hardware and software tools, and it has been applied to a variety of fluid dynamics and computational science problems [1].

Li [13] developed a two-dimensional (2D) AMR method derived from the qualitative theory of differential equations. The AMR method refines a given mesh based on the numerically computed velocity fields. The efficiency and accuracy of the AMR method has been verified using the accurate locations of singular points, asymptotic lines and closed streamlines [12], and against widely used CFD benchmark experiments including the lid-driven cavity flow [11], the 2D unsteady flow past a square cylinder [14], the backward-facing step flow [17] and 2D flow over a wall-mounted plate [16]. In particular, the AMR method has been shown to be useful for capturing localized flow features such as accurate location of the centre of vortices within the refined cells [11, 16]. The AMR method is robust [11], low-cost [15] and can be applied to any incompressible fluid flow [18]. The previous works, for example, [14, 17], considered the accuracy of the 2D AMR method with two refinements and used the finite volume methods. We showed that the twice-refined cells contain the centre of vortices. Since the 2D AMR can be applied a finite number of times, more accurate centre of vortices can be obtained if the numerical velocity fields are accurate enough and more refinements are carried out. The accuracy of the AMR method depends only on the accuracy of the numerical methods used.

Flow around a square cylinder is a classic CFD problem and has been studied by many researchers (see, for example, [7, 8, 19]). The flow pattern characteristics are related to factors such as the Reynolds number (Re) of fluid, the dimension of the square cylinder and the space size. The complex flow characteristics in the vicinity of a square cylinder have always been a focus area and a challenge in academic research. The outcomes of this study can be applied to problems in aerodynamics, wind engineering and electronics cooling. One of the examples is the design of a building. The flow around a building has high- and low-pressure areas. These areas significantly affect building structural integrity, energy efficiency and indoor comfort.

https://doi.org/10.1017/S1446181124000166 Published online by Cambridge University Press

It is noted in the literature that the flow around a square cylinder is steady for $5 \leq Re < 60$ and a fixed blockage ratio of 1/8 [7, 19]. Accordingly, the present study aims to use the AMR method of Li [13] and provide estimates of coordinates of the locations of the centre of vortices for steady incompressible flow past a square cylinder. The AMR method is tested on eight cases considering flows with different Reynolds numbers, that is, $5 \leq Re \leq 50$. Hence, the main contribution of our work is showing the accuracy of the AMR method using four refinements and the finite-element method. Furthermore, we show that the AMR method can capture the location of the centre of vortices within the fourth refined cell. The efficiency of the AMR method in identifying accurate locations of the centre of vortices is validated against the available numerical results found in the literature in which a much finer mesh was used for the study. The methods in the literature investigating flow around a square cylinder (for example, [8]) are limited to steady incompressible flow only. However, the AMR used in this paper can be applied to both steady and unsteady incompressible flows.

The remainder of this paper is structured as follows. Section 2 outlines the methodology, presenting the governing equations, the computational mesh and the flow solver. The numerical results of the eight test cases and the accuracy verification of the 2D AMR method are presented and discussed in Section 3. The conclusion follows in Section 4.

2. Methodology

This section briefly describes the governing equations, the computational domain and the mesh structure, and the flow solver.

2.1. Governing equations We consider the finite-element discretizations of the 2D unsteady, incompressible Navier–Stokes equations [5], which contain the continuity equation and the momentum equations in two directions defined by

$$\nabla \cdot \mathbf{V} = 0,$$
$$\frac{\partial \mathbf{V}}{\partial t} + \mathbf{V} \cdot \nabla \mathbf{V} = -\frac{1}{\rho}\nabla P + \nu \nabla^2 \mathbf{V},$$

where $\mathbf{V} = (u, v)$ denotes the velocity field in 2D with u and v as the velocity components in the x- and y-directions, respectively, ν is the kinematic viscosity, ρ is the fluid density, and P represents the scalar pressure.

2.2. Computational domain and boundary conditions The geometry of the computational domain was set as a 2D rectangular channel with length L and width H, as shown in Figure 1. The two ends of the channel were the inlet and outlet. A square cylinder with a side length of $D = 1$ is placed in the middle of the channel centred on the y-axis such that the blockage ratio of the channel, D/H, equals 1/8. To ensure that the distance from the computational inlet to the cylinder does not influence the accuracy of the numerical solution, an essential inlet location of approximately 10 has

https://doi.org/10.1017/S1446181124000166 Published online by Cambridge University Press

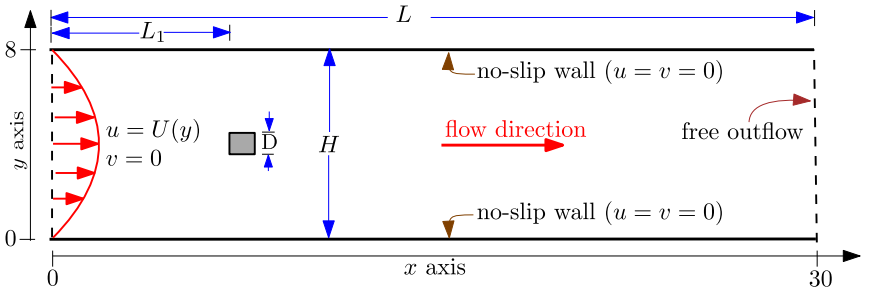

FIGURE 1. Schematic diagram of the computational domain and boundary conditions.

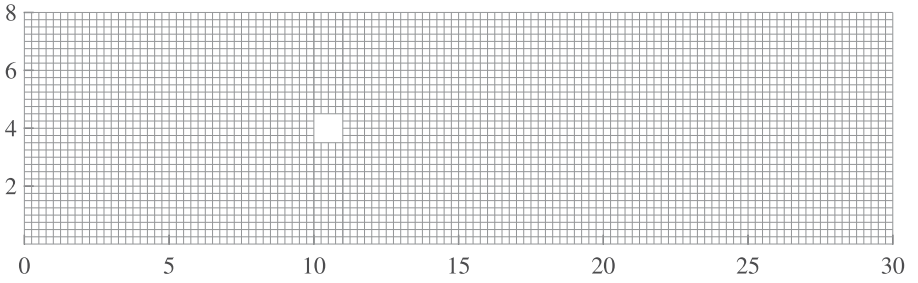

FIGURE 2. The initial mesh (Mesh_0) of 3824 quadrilateral cells with 3984 nodes.

been reported [20]. Thus, we set the inlet length $L_1 = 10$. The channel length L is set to 30.

The boundary conditions used are described in Figure 1. Following [8], the inlet velocity field was specified as a parallel flow with a parabolic horizontal component given by $u = U(y) = 1 - (y - 4)^2/16$. The outlet was set as the free outflow boundary ($P = 0$). The channel's top and bottom boundaries and the square cylinder walls are imposed as rigid surfaces with the no-slip condition ($u = v = 0$). The Reynolds number is considered the main parameter that changes the flow behaviour and is defined as $Re = U_{\max} D/\nu$, where $U_{\max} = 1$ and ν is the kinematic coefficient of the viscosity [8, 19]. Eight test cases for flows with different Reynolds numbers ($Re = 5, 10, 15, 20, 25, 30, 40$ and 50) are considered in this study.

2.3. Computational mesh and the flow solver For all test cases involving different Reynolds numbers, the spatial step size in both the x and y directions is $1/4$. The initial mesh (Mesh_0) has 3824 quadrilateral cells (size $1/4 \times 1/4$) with 3984 nodes. Figure 2 shows the initial mesh Mesh_0. The `Finite Element Analysis simulation Toolbox` (`FEATool`, version 1.16.3, https://www.featool.com/) in `MATLAB` (R2023a) was used to numerically solve the unsteady 2D Navier–Stokes equations [5] for the eight test cases.

This study aims to verify the accuracy of the existing adaptive mesh refinement method with accurate numerical velocity fields. The time-dependent Navier–Stokes

https://doi.org/10.1017/S1446181124000166 Published online by Cambridge University Press

equations are solved using FEATool until both velocity fields and pressures converge to a steady state. The highest-order scheme implemented in FEATool is a second-order implicit Crank–Nicolson time-stepping scheme [6], which was used for the time-dependent settings. We assumed that the convergence is achieved when the numerical solutions (velocity fields) are computed with residuals smaller than 10^{-10} for both u and v. Thus, the time-dependent simulations terminated when either the central processing unit (CPU) time reached the specified simulation time or the normed changes in the dependent solution variables were smaller than the time-stopping criteria (tolerance = 10^{-10}), and at the same time, we make sure velocity fields and pressure show the steady state. Therefore, in this work, only steady-state solutions are considered.

3. Numerical results and accuracy verification

In the present study, we apply the same AMR method from Li and Lal [16]. We refer the reader to the work of Li and Lal [16, Section 3] for a detailed description of the method. A cell-by-cell AMR approach is followed on the quadrilateral meshes. A cell is refined by connecting the mid-points of opposite sides into four equally smaller quadrilateral cells. Applying the AMR method to the initial mesh, Mesh_0, produces the first refined mesh, Mesh_1, and by repeating the procedure three more times, we obtain the fourth refined mesh, Mesh_4. The coordinates of the centre of the isolated refined cells in the area of interest are then used to estimate the centre of vortices.

The results of the eight test cases are presented in this section. We verify the accuracy of the AMR method by comparing it with the reference centre of vortices, $(x_{\text{ref}}, y_{\text{ref}})$, presented by Erturk and Gokcol [8]. There, the authors used the streamfunction and vorticity formulation of the Navier–Stokes equations and employed a very fine mesh with close to 1 040 000 nodes.

3.1. Refined meshes Figure 3 shows the fourth refined mesh (Mesh_4 with 13 223 nodes) for the flow with $Re = 5$. The mesh is refined mostly near the channel's top and bottom boundaries and near the square cylinder.

Figures 4(a)–4(e) show the zoomed-in sections of Mesh_0 to Mesh_4 in the vicinity of the square cylinder for the flow with $Re = 5$. In Mesh_0, a cell to the right of the square cylinder is marked with a red square. The first refinement of the cell marked with a red square is shown in the once-refined mesh, Mesh_1. Similarly, the cell's second, third and fourth refinements are shown in Mesh_2, Mesh_3 and Mesh_4, respectively. Figure 4(f) shows the zoomed-in section of the cell marked with a red square in Mesh_4, which contains an isolated refined cell. The coordinates of the isolated refined cell's centre (X_1, Y_1) are used to estimate the centre of the vortices. The centre is marked with a blue dot in Figure 4(f) for illustration purposes. The marked red boxes in Figure 4(a)–4(e) demonstrate that the AMR method can capture the location of the centre of vortices within the fourth refined cells.

Erturk and Gokcol [8] illustrated that the coordinates of centres of location of the primary vortices are stated from the centre of the square cylinder, as shown in Figure 5.

https://doi.org/10.1017/S1446181124000166 Published online by Cambridge University Press

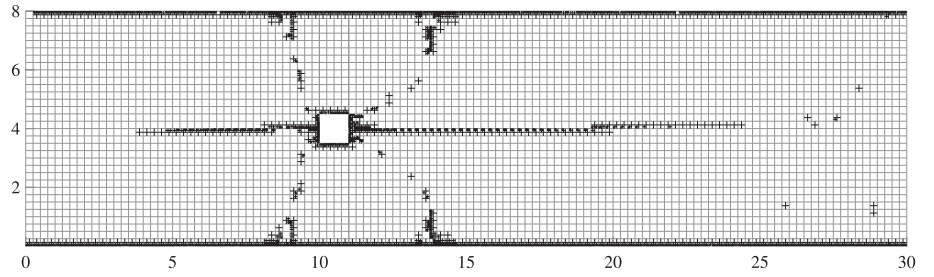

FIGURE 3. Fourth refined mesh, Mesh_4, for the flow with $Re = 5$. Number of nodes = 13 223.

Hence, all estimated coordinates for the centres of vortices, (x_1, y_1), are the results of $(X_1, Y_1) - (10.5, 4)$, where (X_1, Y_1) is the coordinate of the centre of the isolated refined cell. The estimated centre of vortices for the flow with $Re = 5$ is $(x_1, y_1) = (0.609, 0.172)$. We note that the estimated coordinate of the centre of vortices obtained with Mesh_4 is in good agreement with $(x_{\text{ref}}, y_{\text{ref}}) = (0.610, 0.180)$ as reported by Erturk and Gokcol [8].

For the flow with the remaining cases, $10 \leq Re \leq 50$, a similar mesh refinements pattern, as for the flow with $Re = 5$, was observed, for example, Mesh_4 was refined mostly near the channel's top and bottom boundaries, in the vicinity of the square cylinder and the horizontal centre line. It is observed that the x and y values of the coordinates of the centre of vortices gradually increase as the Reynolds numbers increase. The setting for the flows in this study is symmetric, but the refined meshes are not. For all the cases, the lack of symmetry in the refined meshes indicates the nonsymmetrical profile of the velocity field. Hence, the calculated velocity fields are not accurate enough. The number of nodes in Mesh_4 for the flow with $10 \leq Re \leq 50$ ranged from 12 989 to 13 914, which were relatively similar to the case with $Re = 5$.

3.2. Estimated location of centre of vortices Table 1 presents the number of nodes in the fourth refined meshes and the estimated coordinates of vortex centres for the eight test cases. The table also compares the estimated coordinates with the reference centre locations, as reported by Erturk and Gokcol [8]. For each case, the errors $e_x = x_1 - x_{\text{ref}}$ and $e_y = x_1 - y_{\text{ref}}$ were found to be within 5%. The errors relative to the reference vortex centres, computed as

$$\frac{\|(x_1, y_1) - (x_{\text{ref}}, y_{\text{ref}})\|}{\|(x_{\text{ref}}, y_{\text{ref}})\|},$$

were less than 2.5% for all cases. The results obtained by the present method are in good agreement with those obtained by Erturk and Gokcol [8] using a finer mesh. Moreover, we note that further mesh refinements may be needed to obtain coordinates as close as the actual locations of the vortex centres. Figure 6 shows streamline contours and the flow features near the vortex centre for the case with $Re = 5$ and $Re = 50$. The red dots in Figure 6 indicate the location of the centre of vortices.

https://doi.org/10.1017/S1446181124000166 Published online by Cambridge University Press

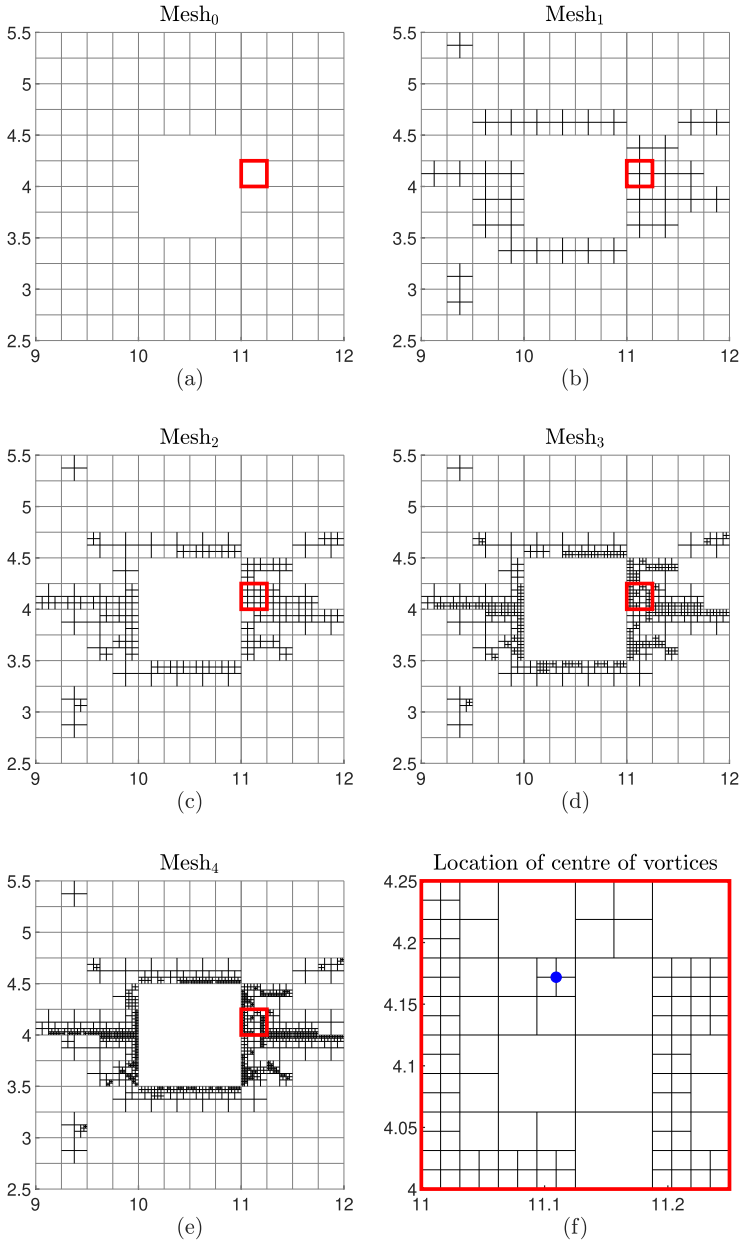

FIGURE 4. Flow with $Re = 5$: (a)–(e) zoomed-in sections of Mesh$_0$ to Mesh$_4$; (f) zoomed-in section of the cell marked with a red square in panel (e), where the blue dot represents the centre of the vortices' estimated location.

https://doi.org/10.1017/S1446181124000166 Published online by Cambridge University Press

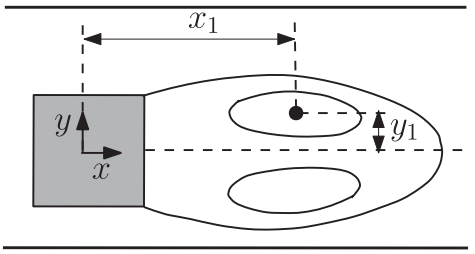

FIGURE 5. Schematic view of the location of coordinates (x_1, y_1) of the primary vortices.

TABLE 1. Number of nodes in Mesh_4, estimated centre locations, (x_1, y_1), and the computed errors relative to the reference vortex centres, $(x_{\text{ref}}, y_{\text{ref}})$. The number of nodes in [8] is approximately 1 040 000.

Re	No. of nodes in Mesh_4	(x_1, y_1)	$(x_{\text{ref}}, y_{\text{ref}})$ [8]	Relative errors
5	13 223	(0.609, 0.172)	(0.610, 0.180)	0.0127
10	12 989	(0.734, 0.203)	(0.740, 0.210)	0.0120
15	13 914	(0.828, 0.234)	(0.840, 0.240)	0.0154
20	13 824	(0.953, 0.261)	(0.940, 0.260)	0.0134
25	13 451	(1.047, 0.266)	(1.030, 0.280)	0.0206
30	13 671	(1.109, 0.291)	(1.120, 0.290)	0.0095
40	13 900	(1.297, 0.328)	(1.300, 0.320)	0.0064
50	13 605	(1.469, 0.344)	(1.490, 0.340)	0.0140

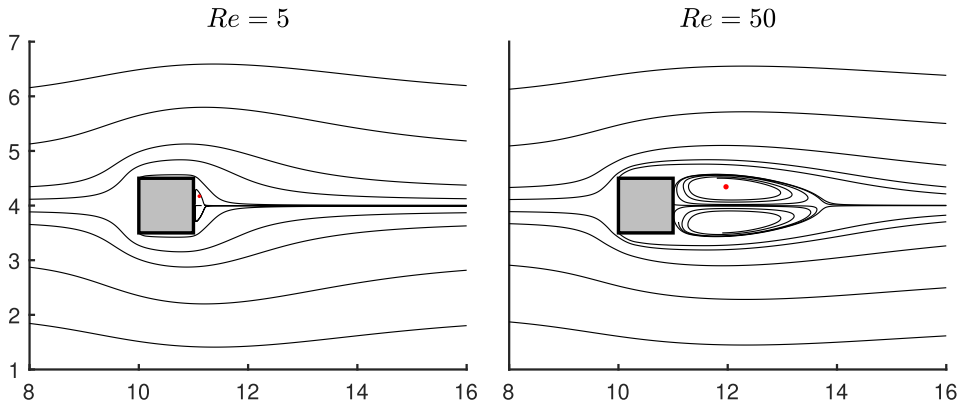

FIGURE 6. Streamline contours. The red dots indicate the estimated vortex location.

4. Conclusion

In this study, we verify the accuracy of the 2D AMR with four refinements using the steady flow past a square cylinder. The accuracy is demonstrated by the estimated location of the centre of vortices contained in the first, second, third and fourth refined

https://doi.org/10.1017/S1446181124000166 Published online by Cambridge University Press

cells. Since the 2D AMR can be applied a finite number of times, we can perform more refinements if the results are not accurate enough for some cases.

References

[1] O. Antepara, N. Balcázar and A. Oliva, "Tetrahedral adaptive mesh refinement for two-phase flows using conservative level-set method", *Internat. J. Numer. Methods Fluids* **93** (2021) 481–503; doi:10.1002/fld.4893.

[2] J. Bell, M. Berger, J. Saltzman and M. Welcome, "Three-dimensional adaptive mesh refinement for hyperbolic conservation laws", *SIAM J. Sci. Comput.* **15** (1994) 127–138; doi:10.1137/0915008.

[3] M. J. Berger and R. J. Leveque, "Adaptive mesh refinement using wave-propagation algorithms for hyperbolic systems", *SIAM J. Numer. Anal.* **35** (1998) 2298–2316; doi:10.1137/S0036142997315974.

[4] M. J. Berger and J. Oliger, "Adaptive mesh refinement for hyperbolic partial differential equations", *J. Comput. Phys.* **53** (1984) 484–512; doi:10.1016/0021-9991(84)90073-1.

[5] J. R. Cannon and G. H. Knightly, "Some remarks on a quasi-steady-state approximation of the Navier–Stokes equation", *ANZIAM J.* **29** (1988) 440–447; doi:10.1017/S0334270000005932.

[6] J. Crank and P. Nicolson, "A practical method for numerical evaluation of solutions of partial differential equations of the heat-conduction type", *Adv. Comput. Math.* **6** (1996) 207–226; doi:10.1007/BF02127704.

[7] A. K. Dhiman, R. P. Chhabra and V. Eswaran, "Flow and heat transfer across a confined square cylinder in the steady flow regime: effect of Peclet number", *Int. J. Heat Mass Transf.* **48** (2005) 4598–4614; doi:10.1016/j.ijheatmasstransfer.2005.04.033.

[8] E. Erturk and O. Gokcol, "High Reynolds number solutions of steady incompressible 2-D flow around a square cylinder confined in a channel with 1/8 blockage ratio", *Int. J. Mech. Eng. Technol.* **9** (2018) 452–463; https://iaeme.com/Home/article_id/IJMET_09_13_047.

[9] H. Friedel, R. Grauer and C. Marliani, "Adaptive mesh refinement for singular current sheets in incompressible magnetohydrodynamic flows", *J. Comput. Phys.* **134** (1997) 190–198; doi:10.1006/jcph.1997.5683.

[10] N. Hannoun and V. Alexiades, "Issues in adaptive mesh refinement implementation", *Electron. J. Differential Equations* **15** (2007) 141–151; https://eudml.org/doc/127549.

[11] R. Lal and Z. Li, "Sensitivity analysis of a mesh refinement method using the numerical solutions of 2D lid-driven cavity flow", *J. Math. Chem.* **53** (2015) 844–867; doi:10.1007/s10910-014-0461-7.

[12] Z. Li, "An adaptive streamline tracking method for two-dimensional CFD velocity fields based on the law of mass conservation", *J. Flow Vis. Image Process.* **13** (2006) 1–14; doi:10.1615/JFlowVisImageProc.v13.i1.10.

[13] Z. Li, "An adaptive two-dimensional mesh refinement method based on the law of mass conservation", *J. Flow Vis. Image Process.* **15** (2008) 17–33; doi:10.1615/JFlowVisImageProc.v15.i1.20.

[14] Z. Li, "Analysis of 2D unsteady flow past a square cylinder at low Reynolds numbers with CFD and a mesh refinement method", *WSEAS Trans. Fluid Mech.* **12** (2017) 150–157; https://wseas.com/journals/articles.php?id=3156.

[15] Z. Li, "Computational complexity of the algorithm for a 2D adaptive mesh refinement method using lid-driven cavity flows", *Comput. Therm. Sci.* **9** (2017) 395–403; doi:10.1615/ComputThermalScien.2017019769.

[16] Z. Li and R. Lal, "Application of 2D adaptive mesh refinement method to estimation of the center of vortices for flow over a wall-mounted plate", *Int. J. Comput. Methods* **20** (2023) Article no: 2143012; doi:10.1142/S021987622143012X.

[17] Z. Li and M. Li, "Accuracy verification of a 2D adaptive mesh refinement method using backward-facing step flow of low Reynolds numbers", *Int. J. Comput. Methods* **18** (2021) Article no: 2041012; doi:10.1142/S0219876220410121.

[18] Z. Li and G. Mallinson, "Simplification of an existing mass conservative streamline tracking method for two-dimensional CFD velocity fields", in: *GIS and remote sensing in hydrology, water resources and environment* (eds C. Yangbo, T. Kaoru, D. I. Cluckie and F. H. D. Smedt) (IAHS Publication, Wallingford, UK, 2004) 269–275; https://iahs.info/uploads/dms/12955.40-269-275-CH-23-Li—Mallinson.pdf.

[19] D. A. Perumal, G. V. S. Kumar and A. K. Dass, "Numerical simulation of viscous flow over a square cylinder using lattice Boltzmann method", *Int. Sch. Res. Not.* **2012** (2012) 1–16; doi:10.5402/2012/630801.

[20] A. Sohankar, C. Norberg and L. Davidson, "Low-Reynolds-number flow around a square cylinder at incidence: study of blockage, onset of vortex shedding and outlet boundary condition", *Internat. J. Numer. Methods Fluids* **26** (1998) 39–56; doi:10.1002/(SICI)1097-0363(19980115)26:1<39::AID-FLD623>3.0.CO;2-P.